Journal of the Serbian Society for Computational Mechanics / Vol. 17 / No. 2, 2023 / pp 104-124
(10.24874/jsscm.2023.17.02.08)

NUMERICAL AND ANALYTICAL PREDICTION OF THE PROPAGATION OF DELAMINATION OF BONDED COMPOSITE REPAIR PLATES UNDER MECHANICAL LOADING

Sofiane Talbi[1*], Mokadem Salem[2], BelaïdMechab[2], Tewfik Ghomari[1], Ahmed Allem[2], Mohammed Khalil Salem[2] and Belabbes Bachir Bouiadjra[2]

[1] Faculty of Engineering and Technology, LAPS Laboratory of Aeronautics and Propulsive Systems, University of USTO, 31000 Oran, Algeria
e-mail: sofiane.talbi@univ-usto.dz, tewfikghomari@yahoo.com
[2] LMPM, Department of Mechanical Engineering, University of Sidi Bel Abbes, BP 89, Cité Ben M'hidi, Sidi Bel Abbes 22000, Algeria
e-mail: moka_salem@yahoo.fr, bmechab@yahoo.fr, sidomed2000@gmail.com, salemkhalil17@gmail.com,bachirbou@yahoo.fr
**corresponding author*

Abstract

This study presents a numerical and analytical prediction of delamination of a repaired joint due to a defect in the composite under tensile loading. The three-dimensional finite element method is used to predict the delamination of a repaired plate with the VCCT method. The effects of the position of the delamination, percentage of the delaminated area, thickness and properties of the patch are presented. It can be noted that the propagation of delamination is significant only at node A and the analyzed model delaminated in mode I. The numerical results are in good agreement compared with the analytical solution found in the literature. It can be seen that the stiffness of the reinforcement material is strongly dependent on the mechanical properties of the patch interface. These results make it possible to choose the carbon/epoxy patch for the repair even if the graphite/epoxy has a high modulus of elasticity. The thickness and the mechanical properties parameter have a significant effect on increasing the durability of the structure.

Keywords: Numerical prediction; bonded composite repair; delamination, fracture mechanics, VCCT method.

1. Introduction

Crack propagation can occur in many structural components of plates and they can also be the cause of premature damage of aircraft. The fracture prediction and the reliability of such structure systems in various practical applications are of primary importance given their impact on the economic plan and security (Mechab et al. 2020; Mechab et al. 2018; Mechab et al. 2014).

The bonded composite repair has been recognized as an efficient and economical method to extend the service life of cracked aircraft structures and the fatigue life of cracked aluminum components was the first otherwise the pioneer of these searches in the aeronautical and maritime research laboratory of the Royal Australian Air Force (Alan Baker, 1993). Several authors (Salem

et al. 2023; Salem et al. 2021; Ibrahim et al. 2018; Bisagni et al. 2013 and Salem et al.2018) analyzed crack growth of the cracked aluminum plates repaired with composite patch. The J-integral fracture parameter has been extensively used in assessing fracture integrity of cracked engineering structures, which undergo large deformation. In the process of stability assessment in structure components, it is important to calculate the point of initiation of the crack and to monitor the subsequent crack propagation behavior (Berrahou et al. 2017; Mechab et al.2016; Serier et al. 2016 and Salem et al. 2019; Baghdadi et at 2019).

Delamination is one of the most disadvantageous fracture modes of stratified composite structures since it can lead to a significant reduction in the load capacity of composite structures (Ravikumar et al. 2017 and Turon et al. 2010). Delamination has varying degrees of impact on the shear strength, fatigue properties, as well as the compressive strength of laminates. De Carvalho et al. (2015), Hosseini Toudesshky et al. (2010), Pa et al. (2021), Fotouhi et al. (2020), Yu et al. (2021), Zhuang et al. (2014) and Azouaoui et al. (2017) presented the propagation of delamination of composite components in aircraft. Kenane and Benzeggagh (1997) studied the Mixed-mode delamination fracture toughness of unidirectional glass/epoxy composites under fatigue loading. The Finite element analysis of the influence of cohesive law parameters on the multiple delamination behaviors of composites under compression (Krueger et al. 2015; Liu et al. 2015; Dàvila et al.2008; Jokinen et al.2019).

This study presents a numerical and analytical prediction of delamination of a repaired joint due to a defect in the composite under tensile loading. The three-dimensional finite element method is used to predict the delamination damage of structure. The effect of the position of the delamination, percentage of delaminated area, patch thickness and properties of patch is presented.

2. Geometric and materials models

The three-dimensional geometrical model used in this study consists of an Al 2024-T3 aluminum plate damaged by cracking and repaired by a simple composite patch illustrated in Fig. 1. The Al 2024 T3 plate is characterized by its height H_p = 600 mm, width W_p = 300 mm and thickness e_p = 2 mm. This plate has a central crack of length “2a” repaired by a multilayer (3 layers) carbon/epoxy composite patch of dimensions H_r = 80 mm, W_r = 160 mm and e_r = 2 mm, i.e. 0.666 mm thick for each layer. The composite patch used is unidirectional with a stacking sequence $[03]_s$, where the plies of the composite are oriented along the length of the plate and in the direction parallel to the loading for all three layers. With the patch bonded to the plate by an FM 73 adhesive of thickness e_a = 0.2 mm, layer 1 is in contact with the adhesive, followed by the layers 2 and 3, respectively. The plate is subjected to a mechanical loading of magnitude σ = 100 MPa. The mechanical properties of the plate, different patch adhesive and mechanical interface properties of different composite materials are shown in Table 1 and Table 2 (Salem M et al. 2015; Turon A et al. 2010; Associates C A E. 2011 ; Goodmiller et al. 2013). For the reasons of symmetry, only one quarter of the structure is modeled.

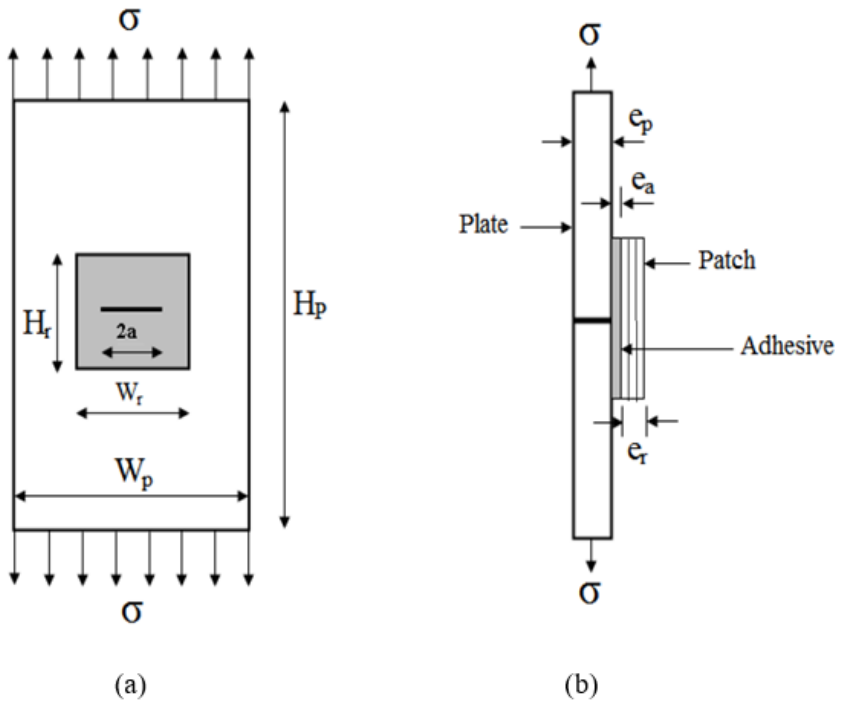

Fig. 1. Geometric model of the analyzed structure: (a) plate without repair; (b) repaired plate seen in profile of the analyzed structure.

	E_1 (GPa)	E_2 (GPa)	E_3 (GPa)	ν_{12}	ν_{13}	ν_{23}	G_{12} (GPa)	G_{13} (GPa)	G_{23} (GPa)
Plate	72			0.3					
Carbon/epoxy	120.0	10.5	10.5	0.3	0.3	0.5	5.25	5.25	3.48
Graphite/epoxy	161.0	11.38	11.38	0.32	0.32	0.45	5.2	5.2	3.9
Glass/epoxy	45.6	16.2	16.2	0.278	0.278	0.4	5.83	5.83	4.5
adhesive FM73	2.55			0.32					

Table 1. Mechanical properties of different materials of the analyzed structure (Salem et al 2018; Turon A et al. 2010; Associates C A E. 2011 ; Goodmiller et al. 2013)

	$G\ I_c$ (kj/m^2)	$G\ II_c$ (kj/m^2)	ŋ
Carbon/epoxy	0,260	1.002	2
Graphite/epoxy	0.212	0.774	2.1
Glasse/epoxy	0.118	2.905	2 .6

Table 2. Mechanical interface properties of different composite materials (Turon. A et al. 2010; Associates C A E. 2011; Goodmiller et al. 2013)

2.1FE Model

The mesh of the structure in a 3D finite element model is shown in Fig. 2. A regular mesh is made for the entire structure. By cubic elements (hexahedra) with eight nodes. The plate is well-partitioned to keep the same mesh throughout the calculation (for different crack sizes) and to avoid any mesh influence on the results. The crack being central leads to a geometric singularity causing stress concentration. Therefore, a refined mesh is made around the crack. The total number of elements in the structure is equal to 28508 and the total number of nodes is equal to 39374, see Table 3.

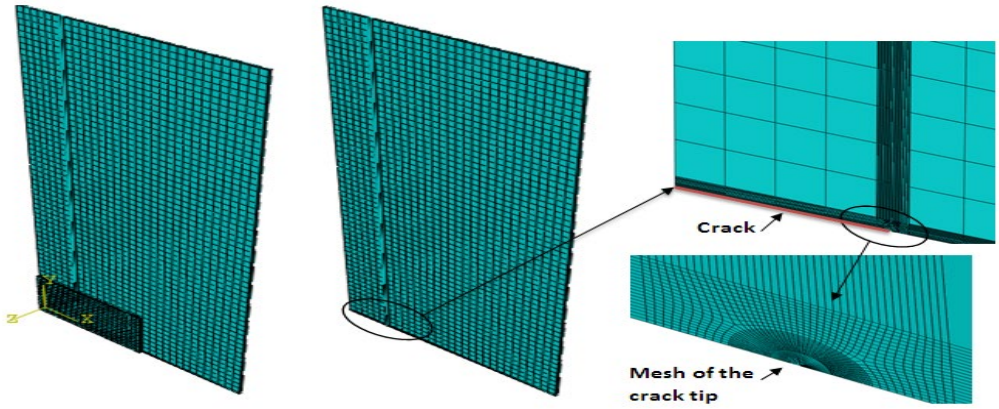

Fig. 2. Mesh of the structure.

by instance	Element type	Number of elements	Number of nodes
Plate AL 2024 T3	C3D8R	25128	32120
Adhesive FM 73	C3D8R	800	1722
layer 1	C3D8R	860	1844
layer 2	C3D8R	860	1844
layer 3	C3D8R	860	1844

Table 3. Number of elements and nodes of the structure.

2.2 Numerical simulation

A delamination defect located at the interface between layers 1 and 2 of the patch, precisely in the center, of rectangular shape with a fixed width of 16 mm and variable length of 12 mm, 24 mm, 48 mm, 72 mm, representing respectively initially delaminated areas worth 1.5 %, 3 %, 6 %, 9 % of the total interface area. The composite patch layers are unidirectional along the height of the plate and in the parallel loading direction. The mechanical properties of the interface for the different types of composite patch are shown in Table 2. The finite element method is used to model delamination as a defect. Layers 1 and 2 of the composite patch are joined by the contact pair surface definition method and the interaction of the delaminated surface is specified with the method “Virtual Crack Closure Technique” (VCCT). In addition, the delamination between the two layers 1 and 2 is modeled by the method Bond nodes in Abaqus Standard. The nodes “A” and “B” are common nodes between layers 1 and 2 representing the outline of the delaminated

area, and the inter-distance "i" is located between the crack front in the plate and the position of node A in the delaminated area in the patch. The interaction between the two layers was simulated by creating arrangements of the master and slave surfaces. The augmented Lagrangian method is performed to reduce the overlap distance of the nodes in contact and to facilitate the resolution of the contact conditions and avoid over-stressing problems (Abaqus /CAE 2021). A schematic representation of the sample is shown in Fig. 3.

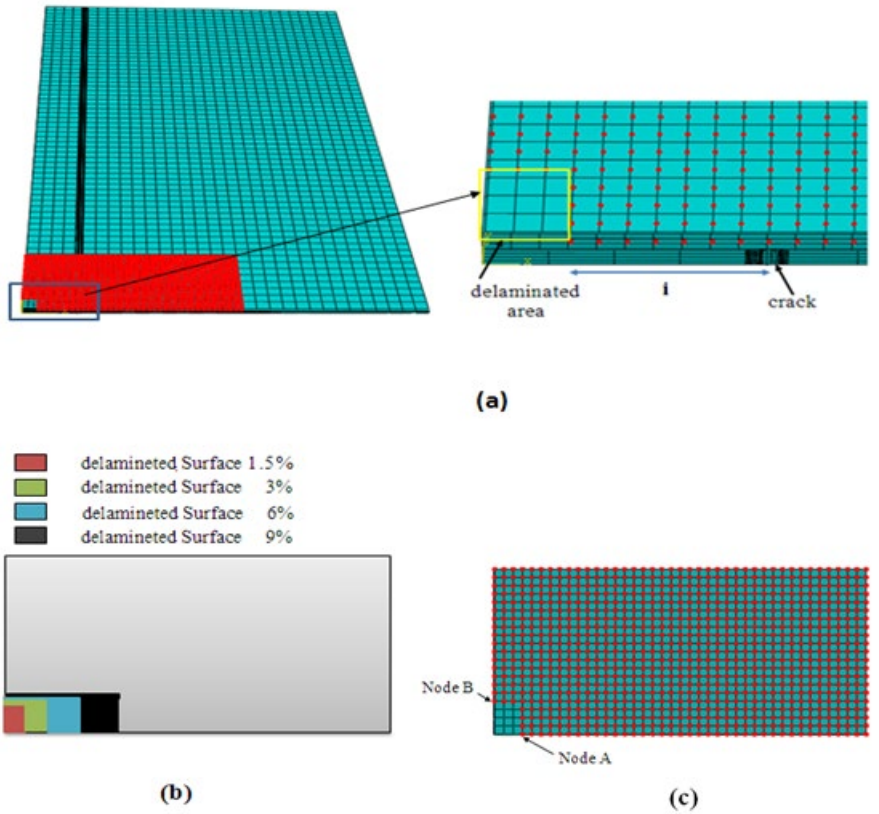

Fig. 3. Schematic representation:(a) central location of delamination and inter-distance i; (b) the interface (layer 1-2) of the patch with different delamination surfaces; (c) The set of nodes representing the considered bonded surface and positioning of nodes A and B.

3. Analytical formulation

3.1 Formulation of the J-integral

Fracture mechanics is the science of studying the behavior of a structure with defects. Conventionally, fracture mechanics assumes that a structure is never flawless. The presence of defects can be in the form of internal cracks or surface cracks such as delamination. In this study, we intend to analyze delamination in modes I and II, which are the most commonly encountered forms of fracture (Fig. 4). The relative displacement field of the crack lips for the two main cracking modes I and II is defined by the following discontinuity (Anh Tuan Tran, 2011):

- Mode I: opening mode:

$$u_1 = 0, u_2(x_1) \neq 0 \tag{1}$$

- Mode II: plane shear mode:

$$u_1(x_2) \neq 0, u_2 = 0 \tag{2}$$

Using the stress field in the singular zone and the linear elastic behavior law, it is possible to relate the rate of energy restitution to the stress intensity factors. The first approach is based on the calculation of stress or strain fields. The second approach considers that crack propagation is an energy dissipation phenomenon. According to Griffith's theory (Anh Tuan Tran, 2011; Associates C A E. 2011), the energy consumed is the difference between the energy state of the system before and after cracking. However, the energy approach has advantages over the stress approach. The rate of energy restitution is relatively easy to determine using analytical methods. This relationship is expressed for the two different modes of cracking by the following formulas (Anh Tuan Tran, 2011; Associates C A E. 2011):

- Mode I: opening mode:

$$J_I = G_I = \frac{\left(K_I^2\right)}{E'} \tag{3}$$

- Mode II: plane shear mode:

$$J_{II} = G_{II} = \frac{\left(K_{II}^2\right)}{E'} \tag{4}$$

- Mixed mode (I, II):

$$G = \frac{\left(K_I^2 + K_{II}^2\right)}{E'} \tag{5}$$

where:

$$\begin{cases} E' = E & \text{in plane stress} \\ E' = \dfrac{E}{1-\nu^2} & \text{in plane strain} \end{cases}$$

with: J: J-integral, G: Energy Release Rate, K: the stress intensity factor (SIF), E: Young's modulus, ν: Poisson's ratio.

The stress intensity factor in modes I and II is calculated from the applied stress 'σ', the geometry of the part and the crack size, in our case represented by the delamination size. The asymptotic value of the SIF has been approximated by Rose (1981) (Anh Tuan Tran.2011) are formally defined by the following formulas:

Mode I:

$$K_I = Y\sigma_{yy}\sqrt{\pi a} \tag{6}$$

Mode II:

$$K_{II} = Y\sigma_{yx}\sqrt{\pi a} \tag{7}$$

with: Y: is a geometric coefficient, for a semi-infinite plate Y= 1.12.

3.2 Formulation of the delamination failure criterion based on the VCCT method

Introduced by Irwin G R. (1960), stress intensity factors correspond to particular kinematics of crack movement. In the framework of linear fracture mechanics, the stresses and strains in the vicinity of a crack admit an asymptotic development whose singular term is written. The stress and displacement fields are expressed using the stress intensity factors:

- In mode I:

$$\begin{cases} \sigma_{xx} = \dfrac{K_1}{\sqrt{2\pi r}}\cos\dfrac{\theta}{2}\left(1-\sin\dfrac{\theta}{2}\sin\dfrac{3\theta}{2}\right) \\ \sigma_{yy} = \dfrac{K_1}{\sqrt{2\pi r}}\cos\dfrac{\theta}{2}\left(1+\sin\dfrac{\theta}{2}\sin\dfrac{3\theta}{2}\right) \\ \tau_{xy} = \dfrac{K_1}{\sqrt{2\pi r}}\cos\dfrac{\theta}{2}\sin\dfrac{\theta}{2}\cos\dfrac{3\theta}{2} \end{cases} \tag{8}$$

$$\begin{cases} u_1 = \dfrac{K_1}{2\mu}\sqrt{\dfrac{r}{2\pi}}\cos\dfrac{\theta}{2}\left(\kappa-1+2\sin^2\dfrac{\theta}{2}\right) \\ u_2 = \dfrac{K_1}{2\mu}\sqrt{\dfrac{r}{2\pi}}\cos\dfrac{\theta}{2}\left(\kappa+1+2\cos^2\dfrac{\theta}{2}\right) \end{cases} \tag{9}$$

- In mode II:

$$\begin{cases} \sigma_{xx} = \dfrac{K_{II}}{\sqrt{2\pi r}}\sin\dfrac{\theta}{2}\left(2+\cos\dfrac{\theta}{2}\cos\dfrac{3\theta}{2}\right) \\ \sigma_{yy} = \dfrac{K_{II}}{\sqrt{2\pi r}}\sin\dfrac{\theta}{2}\cos\dfrac{\theta}{2}\cos\dfrac{3\theta}{2} \\ \tau_{xy} = \dfrac{K_{II}}{\sqrt{2\pi r}}\cos\dfrac{\theta}{2}\left(1-\sin\dfrac{\theta}{2}\sin\dfrac{3\theta}{2}\right) \end{cases} \tag{10}$$

$$\begin{cases} u_1 = \dfrac{K_{II}}{2\mu}\sqrt{\dfrac{r}{2\pi}}\sin\dfrac{\theta}{2}\left(\kappa+1+2\cos^2\dfrac{\theta}{2}\right) \\ u_2 = \dfrac{K_{II}}{2\mu}\sqrt{\dfrac{r}{2\pi}}\cos\dfrac{\theta}{2}\left(\kappa-1-2\sin^2\dfrac{\theta}{2}\right) \end{cases} \tag{11}$$

with:

$$\begin{cases} \kappa = \dfrac{3-\nu}{1-\nu} & \text{in plane stress} \\ \kappa = 3-4\nu & \text{in plane strain} \end{cases}$$

In order to study delamination propagation in the composite patch, based on the VCCT-3D method, using the Irwin hypothesis (Irwin G R. 1960), the strain energy release rate components GI and GII are calculated as the product of the nodal forces at the crack tip and the nodal displacement openings behind the crack tip (Fig. 4). The crack energy fields for the two principal modes of cracking are easily expressed (Associates C A E. 2011) from equations (12) and (13):

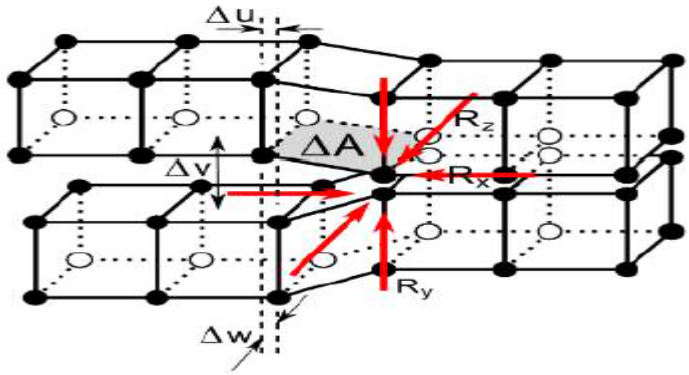

Fig. 4. Forces and nodal openings for 3D geometry.

- Mode I: opening mode:

$$G_I = \frac{1}{2\Delta a} R_Y \Delta v \tag{12}$$

- Mode II: plane shear mode:

$$G_{II} = \frac{1}{2\Delta a} R_X \Delta u \tag{13}$$

The most commonly used fracture criterion in VCCT analyses is the B-K law (Associates C A E, 2011) and it is established in terms of interactions between strain energy release rates as follows:

$$f = \frac{G_T}{G_{I_C} + \left(G_{II_C} - G_{I_C}\right) * \left(\frac{G_{II} + G_{III}}{G_T}\right)^{\eta}} \geq 1.0 \tag{14}$$

$$G_T = G_I + G_{II} + G_{III} \tag{15}$$

with: f: the effective energy release rate ratio, ŋ: the material constant.

4. Validation of the model

In order to validate our numerical results, we have compared in Table 4 the calculated values of the effective energy release ratio of the delamination in the patch with those calculated with the Irwin hypothesis for a crack length of 30 mm of Al 2024 T3 plate, loaded in tension σ = 100 MPa, repaired by a composite patch containing a delamination defect of different size in the interface between layers 1 and 2 of the composite patch. It can be seen from Table 4 that, whatever the size of the delamination in the patch, the relative difference between the numerical and analytical effective energy release ratio does not exceed 4.31 %. We note that the numerical results are in good agreement compared with the analytical solution found in the literature.

Delaminated surface	**Effective energy release rate ratio Analytical**	**Effective energy release rate ratio FEM**	**Relative difference (%)**
1.5%	1,2456	1,19542	4.02%
3%	1,2352	1,1921	4.31%
6%	1,19789	1,15853	3.28%

Table 4. Comparison of FEM results and the analytical solution of Effective energy release rate ratio.

The aim of this section is to validate the results of this numerical approach, and to show that this interface element is capable of correctly simulating the initiation and propagation of delamination in the composite patch. A comparison of the different diagrams presented in Fig. 5 and Fig. 6 shows the ability and the validation of our numerical model to simulate satisfactorily the initiation and propagation of delamination in the composite patch. The present results are in good agreement with the analytical solution the difference is about 2 %

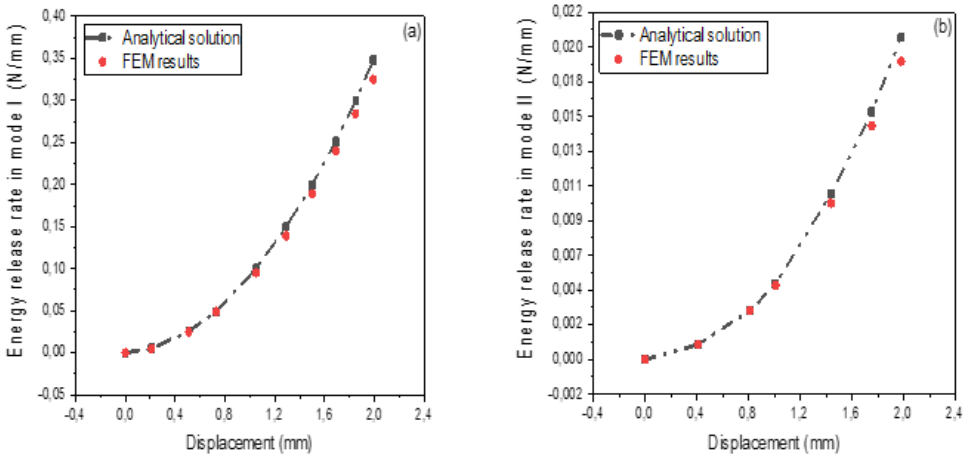

Fig. 5. Comparison of the FEM results and the analytical solution of energy release rate: (a) mode I; (b) mode II.

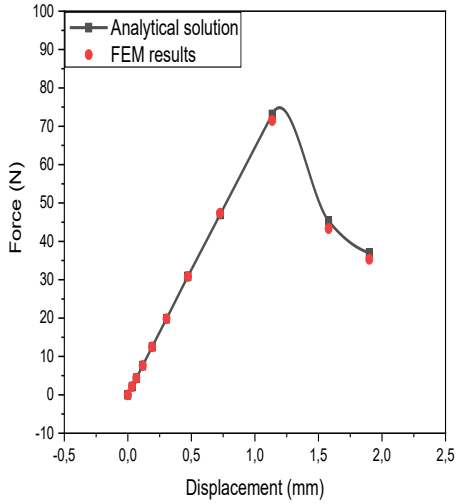

Fig. 6. Comparison of FEM results and the analytical solution of force-displacement diagram in mode I.

5. Results and discussion

5.1 Prediction of the position of the delamination in the repaired plate

The objective of this study is to predict and determine the position of the initiation and propagation of delamination in the interface of layers 1-2 of the patch on the one hand and the most dominant mode of failure on the other. Figure 7 shows the comparative analysis of the variation in the energy release rate on the initiation and propagation of delamination, for an Al

2024 T3 plate with a 30 mm crack repaired by composite patch containing a central delamination surface defect of 3 % in the interface between layers 1 and 2 of the composite patch, with an inter-distance i =18 mm between the crack front in the plate and the delaminated zone in the patch. Figure 7a shows the variation of the energy release rate in mode I at nodes “A” and “B” shown in Fig. 3c. For node “A”, a rapid increase of the energy release rate in mode I is observed for a very short time period until the critical value 0.260 N/mm is reached, beyond t=0.3 s the rate value remains constant. For node “B”, a small increase for a longer time period without reaching the critical value. Figure 7b shows the variation of the energy release rate in mode II in nodes “A” and “B” defined previously (see Fig. 3c). A rapid increase is observed at node “A” for a very short time period until reaching a given constant value clearly below the critical value 1.002 N/mm. For node “B”, the variation is almost zero compared to that obtained for node “A”. The comparative results show that the position of the initiation and the delamination propagation in the interface of layers 1 and 2 of the patch are more important at node “A”.

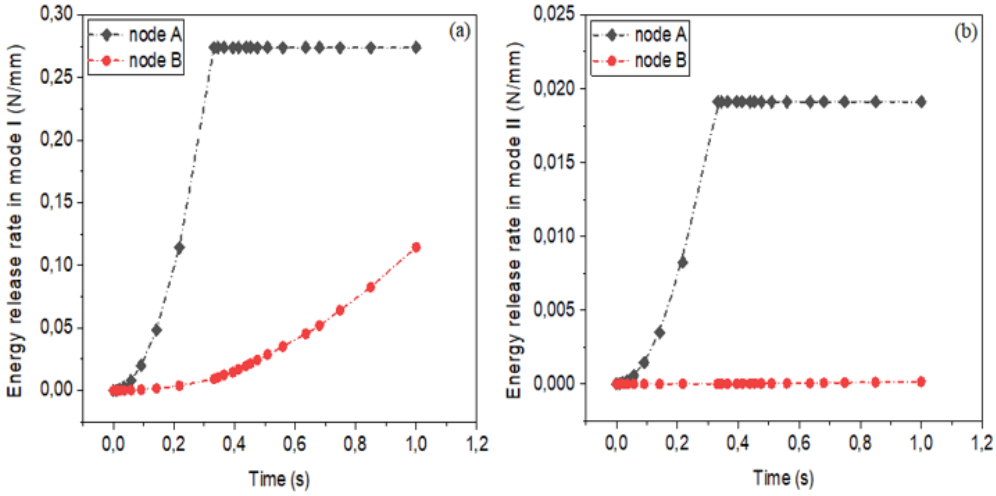

Fig. 7. Variation of the energy release rate at nodes ”A” and “B” for a delaminated area of 3%, a= 30 mm, σ =100 MPa, i=18 mm, (a) in failure mode I, (b) in failure mode II.

Figure 8 shows the comparative analysis of the variation of the energy release rate for the two failure modes I and II on the initiation and propagation of delamination in the interface of layer 1 and 2 at nodes “A” and “B”. From the results obtained, it can be seen that mode I is more dominant than mode II regarding the rate for the two different positions “A” and “B” (see Fig 3c). Moreover, the energy release rate in mode I necessary to initiate delamination reaches the critical value only for node “A”.

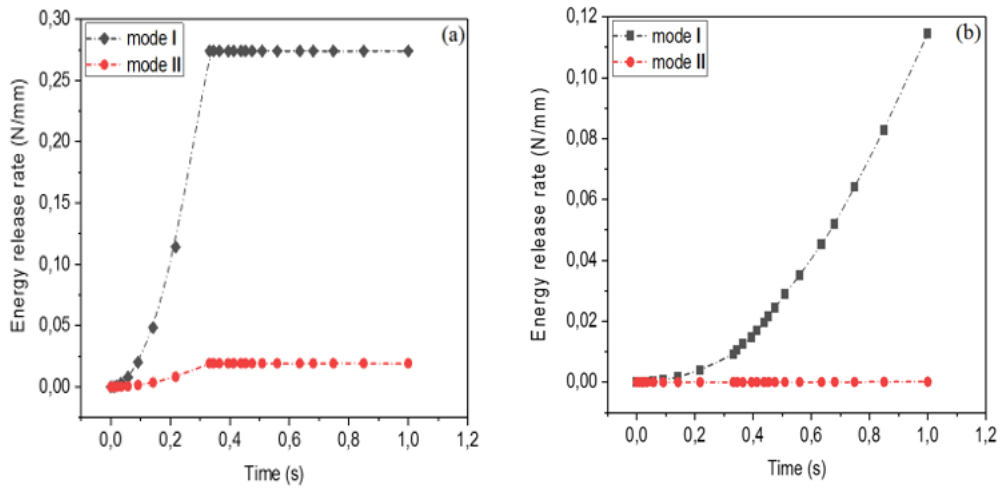

Fig. 8. Variation of the energy release rate in failure mode (I) and (II) for a delaminated surface of 3%, a= 30 mm, and =100 MPa, (a) at node “A”, (b) at node “B”.

The mechanical response and the energy release rate are determining parameters for the initiation and propagation of delamination for the different failure modes. The displacement studied in mode I represents the opening between layers 1 and 2 at the node “A”. The results obtained from these models, in terms of the effect of mechanical response and critical displacement on delamination initiation and propagation for mode I failure in the interface of stack layers 1 and 2, at nodes “A” and “B” (see Fig 3c), are shown in Fig. 9 for a defect of 3 % delamination between layers 1 and 2, and a crack length of 30 mm for an inter-distance "i=18 mm". Figure 9a clearly shows the comparison of the mechanical response at both nodes. At node “A”, the increase corresponds to a linear behavior of the composite patch, until the critical force of rupture value is reached. Beyond this critical value, a drop in force is observed which corresponds to the initiation and propagation of delamination. At node “B”, no increase is observed, which means that there is no delamination propagation in this node. Figure 9b shows the variation of the energy release rate in mode I at nodes “A” and “B” (see Fig 3c). A rapid increase in the rate is observed at node “A” until the critical value "0.260 N/mm" is reached and remains constant. The increase in the rate at node “B” is very insignificant compared to node “A”, and this confirms the validity of the force-displacement curve results obtained in Figure 9a. However, the initiation and propagation of delamination results in a higher sensitivity of the mechanical response in node “A” than in node “B”. It can also be seen that the critical force required to initiate delamination is high in node “A”. Furthermore, the energy release rate required to initiate delamination reaches the critical value only for node “A”. This behavior explains why the initiation and propagation of delamination is significant only at node “A” and that the analyzed model only initiates and delaminates in mode I.

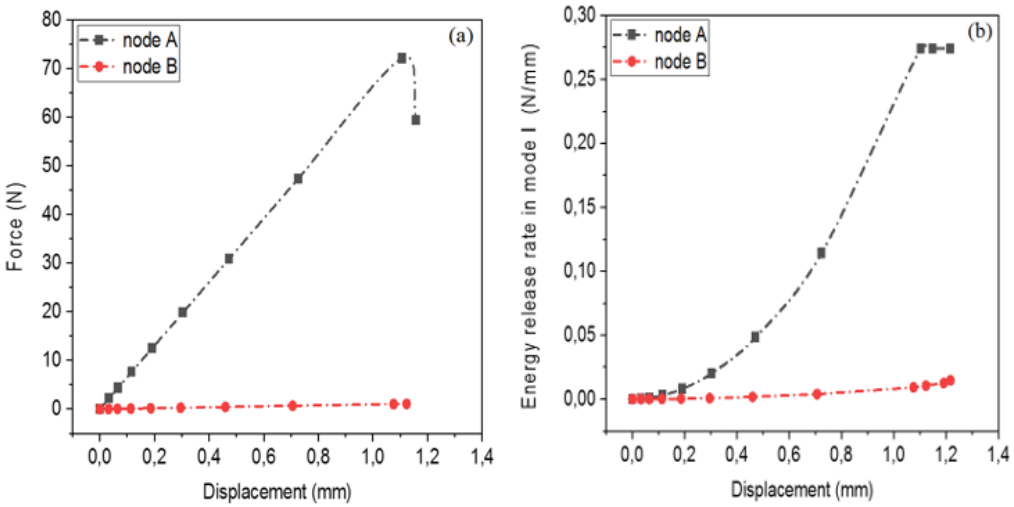

Fig. 9. Descriptive curve: (a) Force – displacement; (b) energy release rate - displacement at nodes "A" and "B" for a delaminated area of 3%, a= 30 mm, σ =100MPa.

5.2 Effect of delaminated surface on repair

This part of the work is part of this context and aims to analyze the effect of defect size on the fracture behavior of the damaged structure repaired by composite patching. Figure 10 shows the effect of delaminated surface size on the repair performance. The variation of the integral-J along the crack front increases as a function of the delaminated area and the crack lengths. The results obtained show that there is an increase in the J-integral at the crack front between a 5 mm and a 15 mm cracked plate which can reach up to 128.48 % for a 1.5 % delaminated area, and 172.6 % for a 9 % delaminated area. For crack sizes 5 mm and 30 mm, and for delaminated areas of 1.5 % and 9 % the increases in the J-integral are 251.49 % and 372.28 % respectively.

On the other hand, the increase in delaminated area leads to an increase in the J-integral, such that for a delaminated area varying between 1.5 % and 9 % the increase in J-integral is 6.78 % for a crack size of 5 mm, 27.4 % for a crack size of 15 mm, and 43.48 % for a crack size of 30 mm. The increase in delaminated area in the composite patch leads to an increase in the value of the J-integral at the crack front. This behavior is normal and is due to the behavior of the composite patch state, i.e. the variation of the J-integral depends strongly on the initial delaminated area. This, during the induced energy transfer from the crack head to the composite patch, causes the initiation and propagation of delamination in the patch. For a repaired cracked plate, the increase in the crack size causes an increase in the J-integral. The presence of a delamination defect in the composite patch further increases the J-integral value.

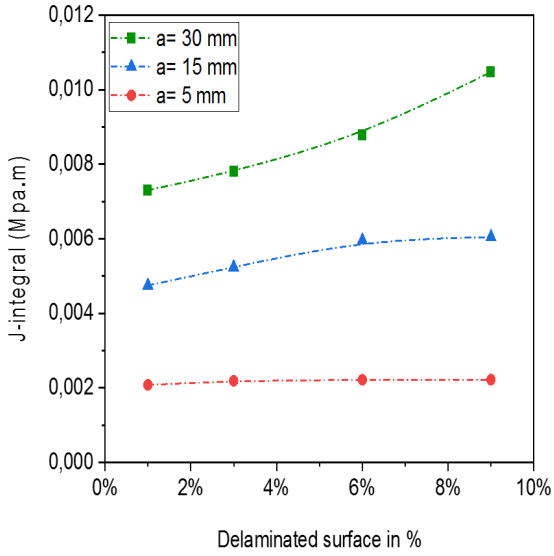

Fig. 10. Variation of integral-J as a function of delamination area for different plate crack lengths, σ =100MPa.

The results obtained, showing the effect of the delaminated surface on the mechanical response, are shown in Fig. 11, for a 30 mm crack and in the presence of a surface delamination defect that varies by 1.5 %, 3 % and 6 %, respectively, for an inter-distance i of 24 mm, 18 mm and 6 mm. Figure 11a shows the variation of the mechanical response at node "A" for different delaminated surfaces on the failure behavior of the damaged structure. The mechanical response at node "A" has a strong dependence on the delaminated surface. For a 1.5 % delaminated surface, the critical force reaches the value of 73.74 N for a displacement of 1.015 mm; for a 3 % delamination the critical force value is 72.08 N and a displacement of 1.10 mm, and for a 6 % delamination the critical force reaches the value of 69.13 N for a displacement of 1.27 mm. It can be seen that in Mode I failure, as the delaminated area increases, the critical force required to initiate delamination decreases, but the displacement increases. Figure 11b shows the effect of delaminated area on the Mode I energy release rate behavior at node "A" (see Fig. 3c) for a crack length of 30 mm and delamination of different areas. This curve shows the variation in energy release rate as a function of mode I displacement for three different delamination surfaces 1.5 %, 3 % and 6 %. It can be seen that the value of the energy release rate increases rapidly until it reaches the critical value, beyond which the value of the rate remains constant. The energy release rate necessary to initiate delamination is reached for large critical displacements, when there is an increase in the delamination area.

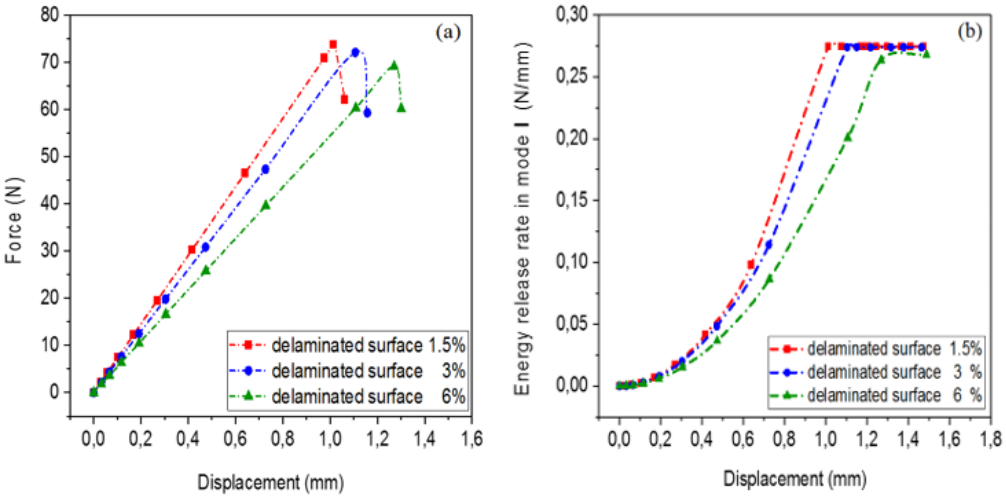

Fig. 11. Descriptive curve: (a) Force – displacement; (b) energy release rate - displacement at node "A" for different delamination surfaces, σ =100MPa, a=30 mm.

5.3 Effect of patch thickness

The objective of this study is to analyze the individual and simultaneous effect of these two parameters of patch thickness and delaminated area on the quality of the repair in terms of reduction of the J-integral at the crack tip. Figure 12 shows the variation of the J-integral along the crack front as a function of the delaminated area, for different patch thicknesses (1 mm, 2 mm, 3 mm), with a 30 mm crack. The performance of this geometric parameter is then analyzed in terms of reductions in the J-integral at the crack front of the plate. It is found that the thickness of the patch introduces a strong influence on the J-integral. A reduction of the J-integral at the crack front for a patch-repaired cracked plate with a thickness of 1 mm and 2 mm containing a surface delamination of 1.5 % can reach up to 65.11 %, and for a composite patch with a surface delamination of 9 % it can reach up to 35.87 %. The same finding when the patch thickness varies from 1 mm to 3 mm, for a 1.5 % surface delamination reaching a reduction rate of the -J integral of about 189.05 %, and 102.96 % for a 9 % delamination.

On the other hand, the increase of the delamination area in the patch leads to an increase of the J-integral. The latter reaches the value of 19.86 %, for a cracked plate repaired by a composite patch of e_r=1 mm thickness, and 45.65 % for e_r=2 mm thickness, and is 70.7 % for a thickness e_r=3 mm, when the delaminated area varies from 1.5 % to 9 %. It can be seen that there is a significant reduction in the J-integral values for an increase in patch thickness. On the other hand, patches containing a delamination defect result in a large increase in the J-integral, leading to delamination repair failure.

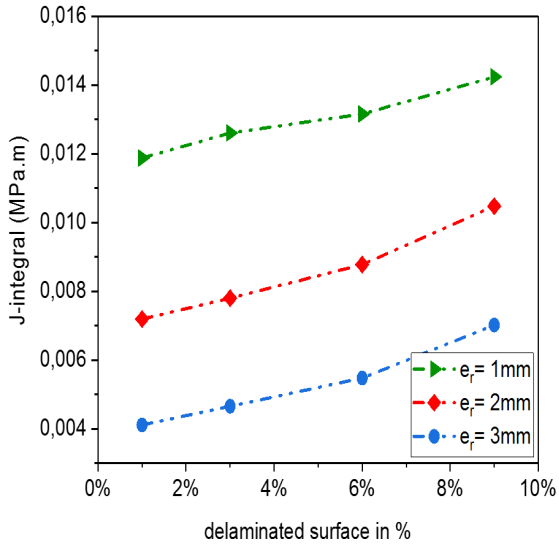

Fig. 12. Variation of integral-J as a function of delamination area for different patch thicknesses, a=30 mm, σ =100MPa.

Figure 13 shows the variation in force and energy release rate as a function of the displacement in mode I between the two layers 1 and 2 of the patch at node "A" (see Fig. 3c) to demonstrate the effect of the interaction of patch thickness and delaminated surface on the initiation and propagation of delamination in the interface, for a=30 mm crack with the presence of a central 3 % delamination defect between layers 1 and 2 with an inter-distance of i=18 mm. The curve shows the variation for three different thicknesses. The energy release rate in mode I reaches the critical value for a critical displacement of about 1.64 mm, 1.10 mm, and 0.8 mm, respectively, for the thicknesses e_r = 1 mm, 2 mm, 3 mm. This variation in the rate is at the origin of the increase in the force until it reaches the critical value of 58 N, 72.08 N, and 85.18 N, respectively, for the same critical displacements defined previously. Beyond this critical value, a constancy in the rate is observed and a drop in the force corresponds to the initiation and propagation of delamination.

The results obtained show that the increase in patch thickness leads to an increase in the critical value of the force required to initiate delamination, while the value of the critical displacement decreases progressively. Furthermore, the energy release rate in mode I required to initiate delamination is achieved at lower critical displacements when the patch is thicker. This can lead to a significant reduction in the performance of structures repaired by composite patches.

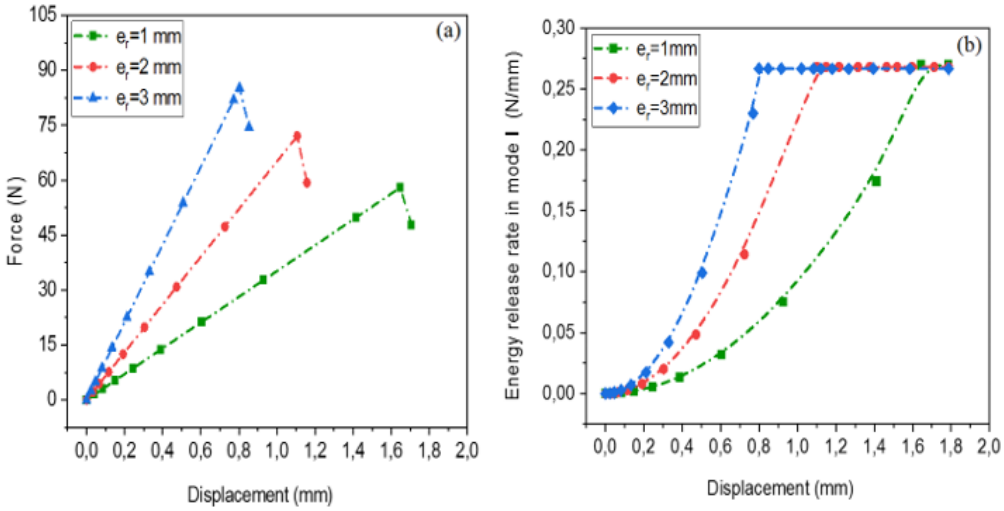

Fig. 13. Descriptive curve: (a) Force - displacement, (b) energy release- displacement at node "A" for different patch thicknesses, σ =100 MPa, a=30 mm and 3% delaminated area.

5.4 Effect of mechanical properties of the patch

The objective of this paper is to perform the repair in terms of crack stability by reducing the J-integral factor, in the presence of a delamination defect in the composite patch. To do this, the repair is carried out using patches of different natures Table 1 and 2and with a central surface defect of 4 % delamination in the interface of layers 1 and 2. The models analyzed differ only in the nature of the repair material.

Figure 14 shows the variation of the J-integral along the crack front of the Al 2024 T3 plate as a function of the delamination area for different natures of the composite patch. The variation of the J-integral depends on the nature of the patch and the delamination area. The reduction of the J-integral at the crack front for a graphite/epoxy patch and a carbon/epoxy patch with 1.5 % and 9 % delamination size, respectively, reaches the values 16.15 % and 12.25 %. In the case of repair by graphite/epoxy patches on the one hand, and glass/epoxy patches on the other hand, for the same delamination areas, the reduction is 59.03 % and 42.03 %.

On the other hand, the increase in the delamination area leads to an increase in the J-integral. For a plate repaired with composite patches of (graphite/epoxy, carbon/epoxy, glass/epoxy), the increase is 48.47 %, 43.48 %, 32.6 %, respectively, when the delamination area varies from 1.5 % to 9 %. The results of the comparative analysis in Figure 14 show that the plates repaired with high strength composite patches, in this case graphite/epoxy, are more reliable and efficient in terms of J-integral reduction. However, this reduction is still not significant due to the presence of a delamination defect in the patch, as this causes a simultaneous increase in J-integral. The results obtained show that the repair becomes more and more effective with the increase of the modulus of elasticity and the interface failure parameter of the composite patch.

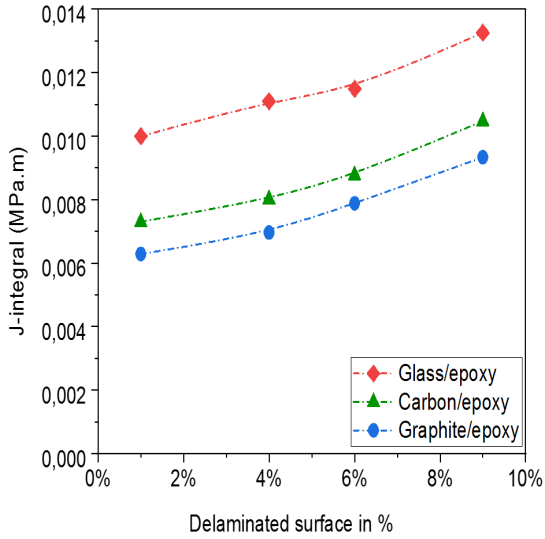

Fig. 14. Variation of J-integral as a function of delamination area for different composite materials with a=30 mm. σ =100MPa.

A numerical study using the finite element method was conducted to analyze the effect of the nature of the composite patch on the damage behavior of initially crack-damaged structures in terms of reducing the initiation and propagation of delamination in the composite patch. For a composite patch containing a surface defect of 4 % delamination and a crack length of 30 mm with an inter-distance "i= 14 mm". Figure 15a shows the variation in force value at node “A” (see Fig. 3c). The analysis of this figure clearly shows that the mechanical response has a different behavior depending on the nature of the patches and the mechanical properties of the interface. For a glass/epoxy composite patch, the critical force reaches its value of 34.61 N for a displacement of 0.63 mm, the graphite/epoxy composite patch the critical force reaches its value of 67.70 N for a displacement of 0.83 mm, and for a carbon/epoxy patch the critical force reaches the value of 71.17 N for a displacement of 0.96 mm. This variation in the previous force corresponding to an increase in the energy release rate in mode I at node “A”, Fig. 15b, this curve shows the variation in the rate in mode I until the critical value for initiating delamination is reached, for three different types of patches (glass/epoxy, graphite/epoxy, carbon/epoxy), respectively, for the same critical displacements defined previously. Above this critical value, a stable value of the rate is observed and a drop in the force corresponds to the initiation and propagation of delamination. The results of the comparative analysis show that the higher the mechanical properties of the interface, the higher the energy release rate in mode I and the force required for delamination initiation. This confirms that the modulus of elasticity is not the only parameter determining performance. It can be seen that the stiffness of the reinforcement material is strongly dependent on the mechanical properties of the patch interface. These results make it possible to choose the carbon/epoxy patch for the repair even if the graphite/epoxy has a high modulus of elasticity.

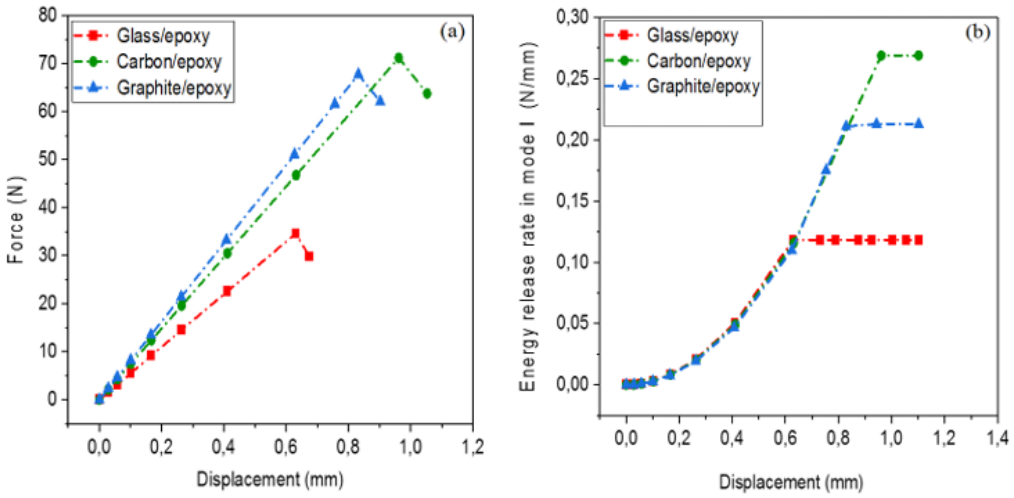

Fig. 15. Descriptive curve: (a) Force - displacement, (b) energy release rate- displacement at node "A" for different patch materials, σ =100 MPa, a=30mm, 4 % delaminated area.

6. Conclusion

A methodology for predicting the propagation of delamination under mixed-mode fracture with VCCT method has been proposed in this study by the three-dimensional finite element method of repaired plate. The effects of the position of the delamination, percentage of delaminated area, thickness and properties of patch have been presented. The numerical results are in good agreement compared with the analytical solution found in the literature. It can be noted that the propagation of delamination is significant only at node "A" and the analyzed model delaminates in mode I, while the presence and increase in the size of the delaminated surface leads to an increase in the J-integral. It can be seen that the stiffness of the reinforcement material is strongly dependent on the mechanical properties of the patch interface. These results make it possible to choose the carbon/epoxy patch for the repair even if the graphite/epoxy has a high modulus of elasticity. The thickness and the mechanical properties parameter have a significant effect on increasing the durability of structure.

References

Abaqus /CAE 2021, Abaqus Standard /user's manual, Dassault systems, Providence, RI, USA.

Alan Baker (1993). Repair efficiency in fatigue-cracked aluminium components reinforced with boron / epoxy patches, Fatig. Fract. Eng. Mater. Struct, 16 (7), 753–765.

Anh Tuan Tran (2011). Etude du délaminage en mode II de composites unidirectionnels soumis à des sollicitations rapides: approche globale et approche locale. Mécanique des matériaux [physics.class-ph]. Arts et Métiers ParisTech.

Azouaoui K and Boumediene T H (2017). Analysede l'amorçage et propagation du délaminage en utilisant un élément d ' interface basé sur la technique de fermeture virtuelle de fissure (VCCT).

Baghdadi M, Serier B, Salem M, Zaoui B, Kaddouri K (2019). Modeling of a cracked and repaired Al 2024T3 aircraft plate: effect of the composite patch shape on the repair performance, Fratt ed Int Strutt, 50 pp 68-85.

Berrahou M, Salem M, Mechab B, Bachir Bouiadjra B (2017). Effect of thecorrosion of plate with double cracks in bonded composite repair, Struct Eng and Mech, Vol 64, pp 323-328.

Bisagni C, Brambilla P, and Dávila C G (2013). Modeling delamination in postbuckled composite structures under static and fatigue loads, Int. SAMPE Tech. Conf, pp .1035 – 1049.

Dávila C G, Camanho P P, and Turon A (2008). Effective simulation of delamination in aeronautical structures using shells and cohesive elements, J. Aircr, vol. 45, (no. 2), pp 663 – 672.

De Carvalho N V, Chen B Y, Pinho S T, Ratcliffe J G, Baiz P M, and Tay T E (2015). Modeling delamination migration in cross-ply tape laminates,Compos. Part A Appl. Sci. Manuf., vol. 71, pp192–203.

Fotouhi M, Damghani M, Leong M C, Fotouhi S, Jalalvand M, and Wisnom M R (2020). "A comparative study on glass and carbon fibre reinforced laminated composites in scaled quasi-static indentation tests," Compos. Struct., vol. 245, p 112 327.

Goodmiller, Geofrey Roy (2013). Investigation of Composite Patch Performance Under Low-Velocity Impact Loading, Master's hesis, University of Tennessee.

Hosseini Toudeshky H, Hosseini S, and Mohammadi B (2010). Delamination buckling growth in laminated composites using layerwise-interface element, Compos. Struct., vol. 92, no. 8, pp 1846–1856.

Ibrahim N C M, Serier B, Mechab B (2018). Analysis of the crack - crack interaction effect initiated in aeronautical structures and repaired by composite patch,Fratt ed Integrità Strut,46, 140-149.

Irwin G. R (1960). "Fracture Mechanics", In Structural Mechanics, ed J. N. Goodier & N. J. Hoff, New York, pp: 557-591.

Jokinen J and Kanerva M (2019). Simulation of Delamination Growth at CFRP-Tungsten Aerospace Laminates Using VCCT and CZM Modelling Techniques, Appl. Compos. Mater, vol. 26,(no. 3), pp 709–721.

Kenane M and Benzeggagh M L (1997). Mixed-mode delamination fracture toughness of unidirectional glass/epoxy composites under fatigue loading, Compos. Sci. Technol., vol. 57, (no. 5), pp 597–605.

Krueger R (2015). The virtual crack closure technique for modeling interlaminar failure and delamination in advanced composite materials. Elsevier Ltd.

Liu P F, Gu Z P, Peng X Q, and Zheng J Y (2015). Finite element analysis of the influence of cohesive law param- eters on the multiple delamination behaviors of composites under compression, Compos. Struct., vol. 131, pp 975–986.

Mechab B, Chama M, Kaddouri K, Slimani D (2016). Probabilistic elastic- plastic analysis of repaired cracks with bonded composite patch, Steel and Comp Struct,Vol 20, pp 1173-1182.

Mechab B, Chioukh N, Mehab B, Serier B (2018). Probabilistic Fracture Mechanics for Analysis of Longitudinal Cracks in Pipes Under Internal Pressure, J of Fail Anal and Pre, Vo 18(6), pp 1643 – 1651.

Mechab B, Serier B, Kaddouri K, Bachir Bouiadjra B (2014). Probabilistic elastic-plastic analysis of cracked pipes subjected to internal pressure loads, Nucl Eng and Des. Vol 275, pp281-286

Mechab B, Medjahdi M, Salem M, Serier B (2020). Probabilistic elastic - plastic fracture mechanics analysis of propagation of cracks in pipes under internal pressure, Frattura Ed Integrita Strutturale, 14(54). pp202-210

Pan X, Jiang Y, Li M, and Su Z (2021). Theoretical and numerical investigation of mode-I delamination of composite double-cantilever beam with partially reinforced arms, Fatigue Fract. Eng. Mater. Struct, vol 44, (no. 12), pp 3448–3462.

Ravikumar P, Santosh B, Praveen B, and Kumar B N (2017). Mode 1 delamination analysis and its comparative study of carbon/ epoxy, graphite/ epoxy and Kevlar/epoxy composite structures using VCCT in Ansys, Int. J. Mech. Prod. Eng. Res. Dev, vol 7 (no. 5), pp 269–278.

Salem M, Mhamdia R, Mechab B & Bachir Bouiadjra B (2023). Effect of the stiffness ratio on the growth of repaired fatigue cracks with composite patch, Mech Based Des of Struct and Mach.

Salem M, Berrahou M, Mechab B, Bachir Bouiadjra B (2021). Analysis of the Adhesive Damage for Different Patch Shapes in Bonded Composite Repair of Corroded Aluminum Plate Under Thermo Mechanical Loading, J Fail.Anal and Preven, 21,1274–1282.

Salem M, Berrahou M, Mechab B, Bachir Bouadjra B. (2018). Effect of the angles of the cracks of corroded plate in bonded composite repair, Fratt ed Integrità Strut, 46, 113 - 123.

Salem M, Mechab B, Berrahou M, Bachir Bouiadjra B, Serier B (2019). Failure Analyses of Propagation of Cracks Repaired Pipe Under Internal Pressure, J of Fail Anal and Pre, Vol 19, pp 212–218.

Serier N, Mechab B, Mhamdia R, Serier B (2016). A new formulation of the J integral of bonded composite repair in aircraft structures Struct Eng and Mech, Vol 58 , pp 745-755.

Turon A, Camanho P P, Costa J, and Renart J (2010). Accurate simulation of delamination growth under mixed-mode loading using cohesive elements: Definition of interlaminar strengths and elastic stiffness, Compos. Struct., vol. 92, no. 8, pp 1857–1864.

Ufklyh U et al (2019), composites collés : état de l'art et analyse de sensibilité methods review and sensitivity analysis.

Yu Z, Zhang J, Shen J, and Chen H (2021). Simulation of crack propagation behavior of nuclear graphite by using XFEM, VCCT and CZM methods, Nucl. Mater. Energy, vol. 29, p 101 063

Zhuang L and Talreja R (2014). Effects of voids on postbuckling delamination growth in unidirectional composites, Int. J. Solids Struct., vol. 51, (no. 5), pp 936–944.